Thermal effects for the doped graphene quantum dots: Cyclic voltammetry

Poonam R. Kharangarh*, Akshay Kumar, Raj K. Sharma, Gurmeet Singh

Department of Chemistry, University of Delhi, Delhi, 110007, India

*Corresponding author, E-mail: poonamkharangarh@gmail.com

Abstract

With an objective to develop electrode materials with high specific capacitance and good stability, we prepared Graphene quantum dot-doped with transition metal of HCl by using a facile hydrothermal at different temperatures (~ 80^0C- 140^0C). Samples were characterized by Raman spectroscopy, Powdered X-ray Diffraction (PXRD), U-V Visible Spectroscopy, and Transmission Electron Spectroscopy (TEM). Raman spectroscopy study reveals intensity ratio alters with changes in temperatures. It was found the variation in size with doped GQDs under different temperature conditions from TEM measurements. The observed blue shifts in the energy gap of HCl doped GQDs at higher temperature are attributed to the strong interaction of GQDs with HCl. Electrochemical studies showed a superior strategy for generating transition metals doped GQDs. The higher electrochemical activity has been originated by using cyclic voltammetry of HCl doped GQDs at 120^0C and is found to be superior electrodes than all other heated samples. The simplicity of synthesized material suggests electrode to understand the charge storage mechanism for commercial applications. Copyright © 2017 VBRI Press.

Keywords: GQDs, HCl, TEM, Raman, cyclic voltammetry.

Introduction

Graphene is a single-atom-thick planar sheet of sp^2 - bonded carbon nanostructure with a large theoretical specific surface area of 2630 m^2g^{-1} and high electrical conductivity [1-4]. Supercapacitors based on electrochemically reduced graphene oxide (ERGO) in aqueous electrolytes using cathodic constant-potential reduction were reported [5, 6]. The pseudo-capacitor uses the fast reversible redox reactions of the cations or changes in oxidation states of the cations in electrode materials during operation at the surface of active materials [7]. A lot of work for electrochemical strategy has further been done for simple and efficient, low-cost, massive scalable and well controllable production of graphene quantum dots (GQDs) which is the fragment of graphene oxide. Firstly, Li *et. al.* [8] reported the electrochemical preparation of GQDs in 0.1 M phosphate buffer solution with a filtration-formed graphene film as the working electrode upon the application of cyclic voltammetry scan. Later in 2011, the same group used N-containing tetrabutylammonium per chlorate (TBAP) in acetonitrile as the electrolyte instead of phosphate buffer solution (PBS). Zhang *et al.* [9] in 2012 prepared GQDs by electrolysis of graphite rod (GR) in alkaline condition of 0.1 M NaOH.

The doping of electronegative atoms, such as nitrogen [10, 11], Phosphorus [12], on carbon surfaces is an effective approach to increase the super capacitance. Fei *et al.* [13] found that Boron- and Nitrogen-Doped GQDs as an efficient electro catalyst for oxygen reduction. The principal of the doping method allows overcoming energy barriers for oxygen functionalities, resulting in the elimination of electrochemically unstable groups. Remaining oxygen groups played a significant role in extra pseudocapacitive effects. These electron rich dopants are found to be improving the charge storage capacitance of GQDs films in supercapacitors. To understand the mechanism of charge storage, it is important to study the pseuocapacitance of inorganic pseudocapacitor electrodes. A number of metal oxides, such as ZnO, SnO_2, Co_3O_4, MnO_2, and RuO_2 have been composited with graphene derivatives to prepare electrodes for supercapacitors compared to the porous carbon based EDL electrode [14]. But due to relatively high cost and low conductivity of metal oxide severely limits their practical application in a large scale. Therefore, to overcome of their limitations in practical applications, we prepare doped GQDs with transition metal of HCl at different temperature as a pseudocapacitor electrode due to its low cost and abundant availability. We developed cathodic/anodic doping approach that substitutes positively/negatively charged atoms onto the electrode of GQDs films with doping of HCl at different temperatures. Therefore, we observed that HCl doped GQDs at 120^0C show higher electro

catalytic activity in a KOH electrolyte and deliver high specific capacitance in comparison to all others. The obtained results challenge the view that variation in temperature during synthesis process is an important step to increase the specific capacitance of pseudocapacitors.

Experimental

Materials

Graphite powder (Graphite India), $NaNO_3$ (98%, Sigma Aldrich), $KMnO_4$, (97%, Sigma Aldrich), KOH ($\geq$85%, Sigma Aldrich), 30% H_2O_2 (Sigma Aldrich), and HCl (($\geq$99%, Sigma Aldrich) were used as received. Double-distilled water (ρ=18.2 $M\Omega\cdot cm$) was used for all experiments during the preparation of GO and HCl doped GQDs.

Material synthesis

Synthesis of graphene oxide: Graphite powder was converted into graphite oxide in accordance with the procedure described by Hummers and Offemann [15]. In brief, 3.0 grams of graphite powder was added to 69 ml concentrated H2SO4 with 1.50 grams $NaNO_3$ dissolved in the solution for rephrase. The mixture was stirred for 1 hour at room temperature. The container was subsequently cooled in an ice-bath followed by slow addition of 9.00 grams of $KMnO_4$ while stirring the contents vigorously by a magnetic stirrer for 15 min. The content was then allowed to warm up to room temperature naturally. Double-distilled water was then added slowly in two aliquots of 138 ml and 420 ml at about 15 min intervals. Subsequently, 7.5 ml of 30% H_2O_2 was added and the colour of the suspension changed from light yellow to brown, resulting in the formation of graphite oxide (GO). The product (GO) was then separated by centrifugation, washed with warm water and ethanol several times and dried at 50 °C for 12 h.

Synthesis of HCl doped GQDs: For preparation of doped HCl-GQDs, 5.95mg of HCl were added together in 10 ml of GO solution & 10 ml of deionized (DI) water. The solution was stirred for 30 min and ultrasonication was carried out in sonicator for another 30 min. The pH was adjusted to 12 with KOH, and the resultant solution was then transferred into a teflon lined autoclave and heated at 80^0C to 140^0C with an interval of 20^0C for 4 h by hydrothermal treatment. Furthermore, this solution was naturally brought down to room temperature and subsequently the GQDs were collected by filtration through a 0.22 µm teflon membrane. The final resultant solution was centrifuged at 4000 rpm before any further characterizations were carried out.

Characterizations

Raman spectra were recorded using a Renishaw spectrometer via microscope system equipped with an Ar^+ laser (λ = 514.5nm). Initial calibration was performed with standard Si film using the 520.5 cm^{-1}

band. UV-Visible absorption spectra of dispersions were recorded on a Perkin Elmer Lambda 35 spectrophotometer, with a slit width of 2 nm and scan speed of 240 nm/min. Transmission Electron Microscope (TEM) was obtained using FEI Technai G2 20 electron microscope operating at 200 kV. Cyclic voltammetry (CV) was collected on a CHI-760C potentiostat - galvanostat instrument. The working electrode (WE) was prepared by dropwise casting on glassy carbon electrode. The electrolyte was 1M KOH solution. The measurement was carried out in a three electrode cell, with a Pt counter electrode and an Ag/AgCl reference electrode in aqueous electrolyte. The CV measurements experiments were conducted in the potential range of -0.2 to 0.8V.

Results and discussion

HCl doped GQDs was synthesized hydrothermally with variation of temperature from 80^0C to 140^0C in a single step as shown in **Fig. 1**.
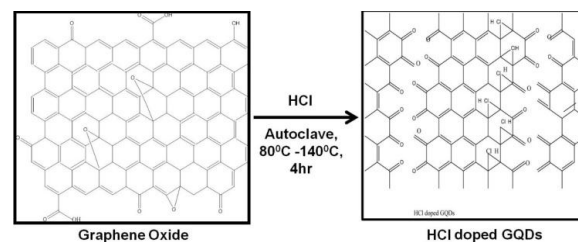
Fig. 1. Schematic of the synthesis of HCl doepd GQDs.

Fig. 2(a)-2(d) show the representative HRTEM images of different samples named as sample 1 (~80^0C), sample 2 (~ 100^0C), sample 3 (~120^0C), and sample 4 (~140^0C). It can be seen that the majority of the sample 3 are in the narrow range of 2.5−7 nm in diameter, is much smaller than 12 nm in diameter of sample 1, 20 nm diameter of sample 2 and 5-7 nm in diameter of sample 4.
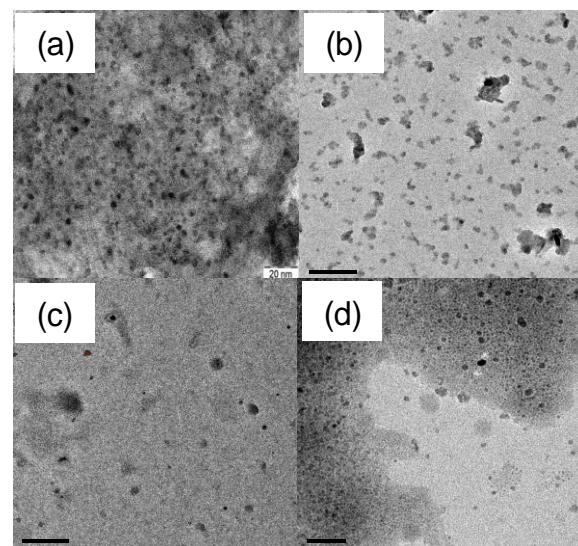
Fig. 2. TEM Images of HCl doped GQDs at (a) 80^0C (b) 100^0C (c) 120^0C and (d) 140^0C.

The optical properties were characterized by Raman spectroscopy to study the changes in GQDs structure after heating for all samples are shown in **Fig. 3**. In all samples, G band (1587 cm^{-1}) and D band (1353 cm^{-1}) were observed with a large intensity ratio of I_D/I_G is 0.97 for sample 2, 0.94 for sample 3, 1.01 for sample 4, which is much lower than that of the original graphene film (~1.05). But sample 1 (I_D/I_G ~ 1.15) gives higher value in comparison to all other samples, even than that of pure graphene film. This intensity ratio indicates that 80^{0}C is not sufficient temperature and 120^{0}C is appropriate temperature to produce high quality GQDs. Samples exhibit a sharper D and G bands suggesting that the intercalation of Cl atoms into the conjugated carbon has led to more structural orders.
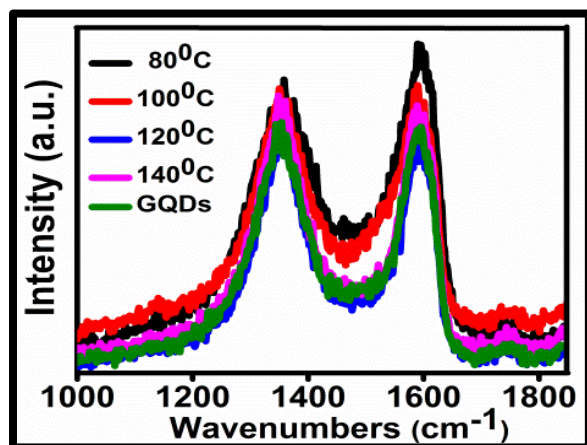
Fig. 3. Evolution of the Raman spectra of HCl doped GQDs at 80^{0}C, 100^{0}C, 120^{0}C, and 140^{0}C.

PXRD measurements were performed to see the crystalline nature as shown in **Fig. 3**. The PXRD pattern of all samples consists of strong reflections at 2θ = 26.43, 43.59 and 54.52º, which are assigned to (111), (220) and (311) planes, respectively indicating a remarkable expansion of graphite due to the presence of oxygen containing functional groups on both sides of graphene sheets and atomic scale roughness arising from sp^3 bonding in carbon [**16,17**].
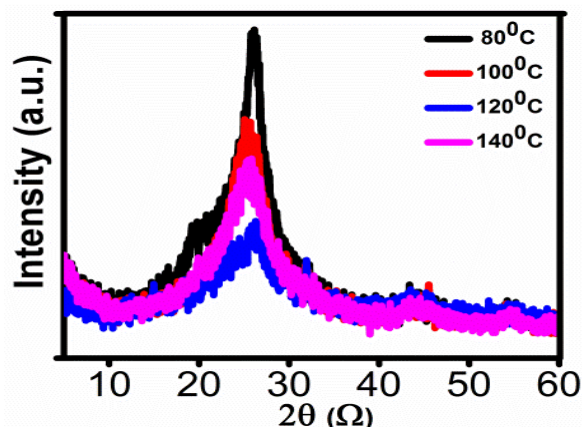
Fig. 4: PXRD pattern HCl doped GQDs at 80^{0}C, 100^{0}C, 120^{0}C, and 140^{0}C.

The (111) reflection is broad with low intensity in sample 3 due to the broken regular stacking and size became smaller.
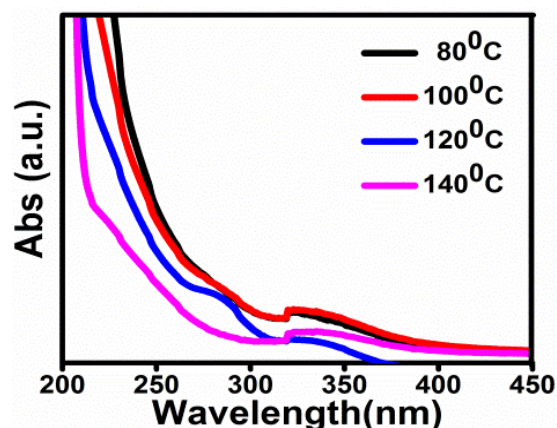
Fig. 5. UV Visible absorption of HCl doped GQDs at 80^{0}C, 100^{0}C, 120^{0}C, and 140^{0}C.

Fig. 5 shows that the UV-visible absorption spectrum of HCl doped GQDs in aqueous solutions. Two absorption peaks 246 nm (5.05 eV) and 318 nm (3.91 eV) were observed in sample1and sample 2 but the spectrum of sample 3 and are characterized by a 230 nm (5.4 eV) and 286 nm (4.34 eV) band. Sample 4 shows the absorption peak at 223 nm (5.56 eV) is resulted from π-π* transitions and 320 nm (3.88 eV) is resulted from n-π* transitions of C=O bond. The presence of functional group state possibly related to oxygen in between valence band (π band) and conduction band (π* band). After the treatment of HCl, the new two blue shifted peaks are observed at 253 nm (4.9 eV) and 298 nm (4.16 eV). The blue shift (or increase in band gap) may be due to the localization of electron-hole pairs of the isolated sp^2 hybridized clusters with obtained small size carbon oxygen matrix.

Electrochemical study

The electrochemical study was done by cyclic voltammmetry (CV) for HCl doped GQDs electrode at different temperatures as shown in **Fig. 6(a-d)**. CV curves were used to observe the charge storage mechanism for HCl doped GQDs electrode. HCl doped GQDs electrodes in the KOH electrolyte can show fast and reversible redox reactions. When HCl doped GQDs electrodes were dipped in KOH electrolyte, it reacts with KOH due to strong electronegativity of OH$^-$ groups present in GQDs. From CV measurements, cathode and anode peaks are observed in HCl doped GQDs at different temperatures for different scan rates. All samples except in sample 2 give a peak at 0.25 V (anodic Peak) and 0.1 V (cathodic peak). But during the scanned in HCl-GQDs at 100^{0}C, a shift in the potential at 0.6 V is there. The cathode peak shifts towards more positive potentials is due to the presence of oxygen functionalities

The anodic peaks (positive current) and cathodic peaks (negative current) in the CV curves originates from the oxidation and reduction process of chlorine, which indicate that the capacitance characteristics are governed by Faradic redox reactions. The anodic peak occurred at 0.1 V, indicating an oxidation state related to Cl (I) → Cl (II) and cathodic peaks correspond to a reduction process following the faradic reduction reactions from Cl (II) → Cl (I). The non-rectangular shapes of CV curves reveal that the charge storage is a characteristic of the pseudocapacitance process originating from the reversible redox reactions of cation. Much work needs to be done to improve the electrochemical performance of pseudocapacitors. Our work of HCl doped GQDs at 120^0C can be appropriate temperature to design for higher capacitance pseudocapacitors.

The scan rate also possesses notable impact in the rate and kinetics of electrochemical reaction as shown in **Fig. 6(a)-6(d)**. When scan rate was varied in the range 20 mV-80 mV/s, there was a corresponding change observed in the current density. The steady increment in the current density along with the scan rate is in agreement with the earlier reported [18].
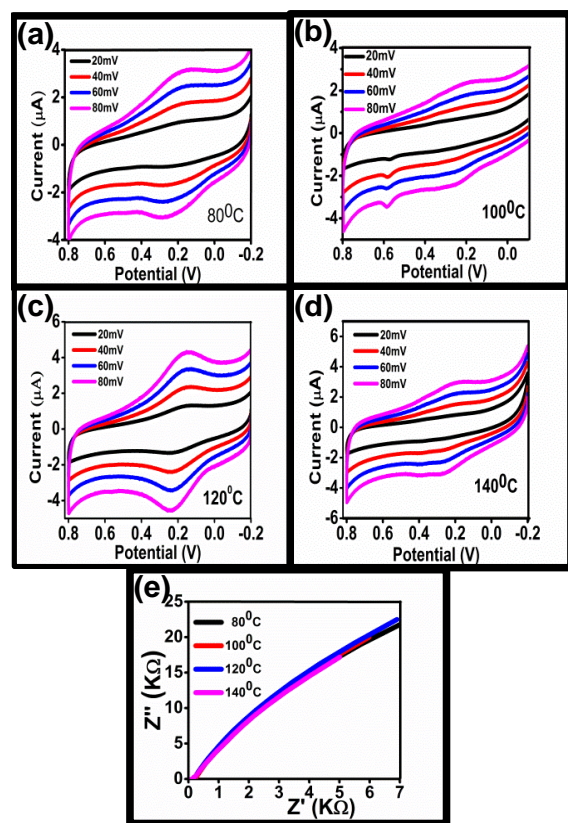
Fig. 6. Cyclic voltammetric analysis of HCl-GQDs (a) 80^0C (b) 100^0C (c) 120^0C (d) 140^0C, and (e) Nyquist plot to all samples.

It has been seen that the deviation of the stability of the first cycle and 100 cycles are negligible confirming the electrochemical cyclic stability of different doped GQDs. From the cyclic voltammetry

experiments, we observed that the specific capacitance of all samples is 34 μF, 33 μF, 5 5μF, and 37 μF for 100 mV. The capacitance of sample 3 is much larger than all other samples

The capacitance can be find out by using the equation given below.

$$C_m = \frac{\left|Q_f\right| + \left|Q_b\right|}{2m\Delta V} \tag{1}$$

The good specific capacitance of GQDs is due to the successive faradic reactions of the HCl functionalities of doped GQDs and surface activation of grapheme sheets by the deoxygenation reaction of doped GQDs in an aqueous solution. In conclusion, the observed peak at 0.25 V is attributed to the electron transfer through conduction and valence band edges of transition metals with GQDs. **Fig. 6(e)** shows that the Nyquist plot (Z' vs. Z") for all samples. For an ideal double layer capacitor, Nyquist plot for low frequency region is a straight line. The more vertical the line, the more closely the supercapacitor behaves as an ideal capacitor [1]. In general, a single semicircular arc is observed [19] which confirm the presence of bulk effects only. In this study, all the samples do not show semicircle, show the superior rate performance for doped GQDs.

Conclusion

The electrochemical performances of all samples were examined by cyclic voltammetry to see the capacitive behavior using a three - electrode configuration by using a simple hydrothermal method. It was observed that the surface redox behavior occur which contribute a pseudo capacitive mechanism to the charge storage at the electrode. The overall performance of doped GQDs at 120^0C was shown superior to that of electrodes than all other samples heated at different temperatures.

Author's contributions

Conceived the plan: G. Singh and R. K. Sharma; Performed the expeirments: P. R. Kharangarh and A. Kumar; Data analysis: P. R. Kharangarh and; Wrote the paper: P. R. Kharangarh and. Authors have no competing financial interests.

References

1. Stoller, M. D.; Park, S.; Zhu, Y; An J, Ruoff, R. S.; *Nano Lett.*, **2008**, *8*, 3498.
2. Yang, J.; Deng, S. Y.; Lei, J. P.; Ju, H. X.; Gunasekaran, S.; *Biosens. Bioelectron.*, **2011**, *29*, 159.
3. Tiwari, A.; Kobayashi, H. (Eds.); Responsive Materials and Methods; Wiley: USA, **2013**.
4. Kitai, A. (Eds.); Luminescent Materials and Applications; Wiley: USA, **2008**.

5. Sun, A.; Zheng, J.; Sheng, Q.; *Electrochem. Acta*, **2012**, *65*, 64.
6. Peng, X. Y.; Liu, X. X.; Diamond, D.; Lau, K. T.; *Carbon*, **2011**, *49*, 3488.
7. Conway, B. E., Klumer-Academic: New York, **1999**.
8. Li, Y.; Hu, Y.; Zhao, Y.; Shi, G.; Deng, L.; Hou, Y.; Qu, L.; *Adv. Mater.*, **2011**, *23*, 776.
9. Zhang, M.; Bai, L.; Shang, W.; Xie, W.; Ma, H.; Fu, Y.; Fang, D.; Sun, H.; Fan F. L.; Han H. M.; Liu, C.; Yang, S.; *J. Mater. Chem.*, **2012**, *22*, 7461.
10. Wang, X. R.; Li, X. L.; Zhang, L.; Yoon, Y.; Weber, P. K.; Wang, H. L.; *Science*, **2009**, *324*, 768.
11. Hulicova, D.; Yamashita, J.; Soneda, Y.; Hatori, H.; Kodama, M.; *Chem. Mater.,* **2005**, *17*, 1241.
12. Hulicova, D.; Puziy, A. M.; Poddubnaya, O. I.; Surez-Garcı́a, F.; Tascn, J. M. D.; Lu, G. Q.; *J. Am. Chem. Soc.* **2009**, *131*, 5026.
13. Fei, H.; Ye, R.; Ye, G.; Gong, Y.; Peng, Z.; Fan, X.; Samuel, E.L.; Ajayan, P.M.; Tour, J.M.; *ACS Nano*, **2014**, *8*, 10837.
14. Candelaria, S.L.; Shao, Y.; Zhou, W.; Li, X.; Xiao, J.; Zhang, J.G.; Wang, Y.; Liu, J.; Li, J.; Cao, G.; *Nano Energy*, **2012**, *1*, 195.
15. Hummers, W. S.; Offeman R. E.; *J. Am. Chem. Soc.*, **1958**, *80*, 1339.
16. Mattevi, C.; Eda, G.; Agnoli, S.; Miller, S.; Mkhoyan, K. A.; Celik, O.; Mastrogiovanni D.; Granozzi G.; Garfunkel E., Chhowalla M.; *Adv. Func. Materials*, **2009**, *19*, 2577.
17. Pimenta, M. A.; Dresselhaus, G.; Dresselhaus, M. S.; Cançado, L. G.; Jorio, A.; Saito, R.; *Phys. Chem. Chem. Phys.*, **2007**, *9*, 1276.
18. Sivakumar, P.; *Electrochimica Acta*, **2014**, *138*, 302.
19. Khurana, G.; Kumar, N.; Kooriyattil, S.; Katiyar R. S.; *J. Appl. Phys.*, **2015**, *117*, 17E106.